



Anti-viral Drug Treatment: Dynamics of Resistance in Free Virus and Infected Cell Populations

MARTIN A. NOWAK[†], SEBASTIAN BONHOEFFER[†], GEORGE M. SHAW[‡]
and ROBERT M. MAY[†]

[†] *Department of Zoology, University of Oxford, South Parks Road, OX1 3PS, Oxford, U.K.*
and [‡] *Division of Hematology/Oncology, University of Alabama at Birmingham, 613
Lyons-Harrison Research Building, Birmingham, Alabama 35294, U.S.A.*

(Received on 25 July 1996, Accepted in revised form on 24 October 1996)

Anti-viral drug treatment of infections with the human immunodeficiency virus type 1 (HIV-1) usually leads to a rapid decline in the abundance of plasma virus. The effect of single drug therapy, however, is often only short-lived as the virus readily develops drug-resistant mutants. In this paper we provide analytic approximations for the rate of emergence of resistant virus. We study the decline of wildtype virus and the rise of resistant mutant virus in different compartments of the virus population such as free plasma virus, cells infected with actively replicating virus, long-lived infected cells and cells carrying defective provirus. The model results are compared with data on the rise of drug-resistant virus in three HIV-1 infected patients treated with zidovudine (ZDV). We find that the half-life of latently infected cells is between 10 and 20 days, whereas the half-life of cells with defective provirus is about 80 days. We also provide a crude estimate for the basic reproductive ratio of HIV-1 during ZDV therapy.

© 1997 Academic Press Limited

1. Introduction

In recent years, a number of anti-viral drugs have been developed that are potent inhibitors of HIV-1 replication *in vivo*. The two major types of anti-HIV drugs are reverse transcriptase inhibitors and protease inhibitors. Reverse transcriptase inhibitors prevent the infection of new cells by blocking the reverse transcription of the HIV RNA into DNA, which would integrate into the host cell genome. Protease inhibitors prevent already infected cells from producing infectious virus particles.

Treatment with either type of drug leads to a rapid decline in plasma virus and an increase in CD4 cells, which constitute the major target cell of HIV infection. Monitoring the rate of virus decline in the first few days of treatment leads to interesting insights into the short-term dynamics of HIV infection. Most of the plasma virus is produced by HIV-infected cells that have a half-life of about 2 days (Ho *et al.*, 1995; Wei *et al.*, 1995; Coffin, 1995; Nowak *et al.*, 1995;

Perelson *et al.*, 1996). The half-life of free virus particles has been estimated to be about 6 hr and the time-span between infection of a cell and production of new virus particles to be around 0.9 days (Perelson *et al.*, 1996). The latter estimates rely on a detailed kinetic understanding of the initial shoulder of virus decline within 48 hr after start of therapy and are therefore problematic (Herz *et al.*, 1996).

Prolonged treatment with a single anti-HIV drug almost always results in the emergence of resistant virus (Larder *et al.*, 1989, 1993, 1995; Larder & Kemp, 1989; Richman, 1990, 1994; Richman *et al.*, 1994; St Clair *et al.*, 1991; Ho *et al.*, 1994; Loveday *et al.*, 1995; Markowitz *et al.*, 1995). In AZT treatment, a number of mutations have been described that render the virus more and more resistant against the drug (Boucher *et al.*, 1990, 1992a, b; Mohri *et al.*, 1993; de Jong *et al.*, 1996). In NVP and 3TC treatment, single point mutations appear to confer high level resistance against the drug

(Richman *et al.*, 1994; Schuurman *et al.*, 1995; Wei *et al.*, 1995). Much hope is currently being offered by combining several different anti-HIV drugs. Simultaneous treatment with AZT and 3TC, for example, can suppress virus load about ten-fold in patients treated for up to 1 year (Eron *et al.*, 1995; Staszewski, 1995). Preliminary data on treatment with AZT, 3TC and a protease inhibitor suggest that virus load can be suppressed to undetectable levels (about a 10000-fold reduction) and stays below detection limit in patients treated for several months (David Ho, Douglas Richman, personal communication).

Mathematical models have been developed to describe the population dynamics of virus replication following drug treatment and the emergence of resistant mutant. McLean *et al.* (1991) proposed that the short term effect of AZT treatment is due to the predator-prey like interaction between virus and host cells, and that the CD4 cell increase following drug treatment is responsible for the resurgence of virus even in the absence of resistant mutants. Nowak *et al.* (1991) study the effect of drug treatment on delaying progression to disease. McLean & Nowak (1992) postulate that the rise of drug-resistant virus is caused by the increase in available target cells for HIV infection. Frost & McLean (1994) and McLean & Frost (1995) describe models for the sequential emergence of resistant variants in AZT therapy. Wein *et al.* (1996) use a control theoretic approach for multidrug therapies. Kirschner & Webb (1996) study the emergence of drug resistant virus in a model with CD4 and CD8 cells. De Boer & Boucher (1996) propose that reducing CD4 cell numbers can potentially prevent the emergence of drug-resistant virus.

In this paper we develop analytic solutions for the emergence of resistant virus under single drug therapy. We will describe the rate of increase of resistant virus in the free virus population and in the infected cell population and show how the model can be used to estimate demographic parameters of virus population dynamics *in vivo*.

In Section 2 we outline the basic model of virus dynamics, in Section 3 we discuss the initial viral decline after start of therapy and in Section 4 we derive analytic approximations for the rise of resistant mutant. In Section 5 we expand the basic model to include cells that harbour latent or defective virus. We present clinical data on three patients treated with NVP in Section 6 and conclude in Section 7.

2. The Basic Model

In the basic model of viral dynamics we distinguish three variables: uninfected cells x , infected cells y , and

virus particles v . Let us assume that uninfected cells are produced at a constant rate, λ , from a pool of precursor cells and die at rate dx . This is the simplest possible host cell dynamics. Later we will discuss more complex assumptions. Virus reacts with uninfected cells to produce infected cells. This happens at rate βxv . Infected cells die at rate ay . Virus is produced from infected cells at rate ky and dies at rate uw . This gives rise to the following system of ordinary differential equations:

$$\begin{aligned}\dot{x} &= \lambda - dx - \beta xv \\ \dot{y} &= \beta xv - ay \\ \dot{v} &= ky - uv.\end{aligned}\quad (1)$$

If the basic reproductive ratio of the virus,

$$R_0 = \beta \lambda k / (adu), \quad (2)$$

is larger than one, then the system converges to the equilibrium

$$x^* = \frac{au}{\beta k} \quad v^* = \frac{\lambda k}{au} - \frac{d}{\beta} \quad y^* = \frac{\lambda}{a} - \frac{du}{\beta k}. \quad (3)$$

3. Viral Decline Under Drug Therapy

Let us assume that the virus infection is in equilibrium (steady state) as specified by eqn (3). We are interested in the decline of free virus and infected cells and the rise of uninfected cells following drug treatment. If a drug prevents the infection of new cells (i.e. $\beta = 0$) then the equations become

$$\begin{aligned}\dot{x} &= \lambda - dx \\ \dot{y} &= -ay \\ \dot{v} &= ky - uv\end{aligned}\quad (4)$$

subject to the initial conditions x^* , y^* , and v^* at $t = 0$. This gives rise to the following solutions:

$$x(t) = \frac{\lambda}{d} - \left(\frac{\lambda}{d} - x^* \right) e^{-dt} \quad (5)$$

$$y(t) = y^* e^{-at} \quad (6)$$

$$v(t) = v^* \frac{ue^{-at} - ae^{-ut}}{u - a}. \quad (7)$$

The initial slope of the rise of uninfected cells is simply $\lambda - dx^*$. Thus for the same value of λ and d , patients with low x^* should have the higher initial decrease. The rise of uninfected cells in the absence of viral resurgence would then level out converging to the uninfected equilibrium, $x = \lambda/d$.

Infected cells fall purely as an exponential function of time. In the applications we have in mind, u is much larger than a ($u \gg a$). For this case, virus density does not begin to fall significantly until $t \approx 1/u$, and thereafter falls as e^{-at} (if $a \gg u$ the converse of course is true).

4. Emergence of Resistant Mutant Under Drug Therapy

In HIV-1 infection there is rapid development of resistant virus to all known drugs. Often a single point mutation can greatly reduce sensitivity to a particular drug. In this section we calculate the rate at which the abundance of a resistant mutant rises. Before drug therapy the resistant mutant virus is held in a mutation-selection balance. It is continuously generated by the sensitive wildtype, but has a slight selective disadvantage. (If it did not have a selective disadvantage it would already dominate the virus population before therapy is given. This is not observed.) An appropriate system that describes this mutation-selection process is the following:

$$\begin{aligned}\dot{x} &= \lambda - dx - \beta xv - \beta_m xv_m \\ \dot{y} &= \beta(1 - \epsilon)xv - ay \\ \dot{v} &= ky - uv \\ \dot{y}_m &= \beta\epsilon xv + \beta_m xv_m - ay_m \\ \dot{v}_m &= k_m y_m - uv_m.\end{aligned}\quad (8)$$

Here y_m describes cells infected by mutant virus, whereas v_m denotes mutant virus particles. The parameter ϵ denotes the probability of mutation from wildtype to resistant mutant during reverse transcription of viral RNA into proviral DNA. If wildtype and mutant differ by a single point mutation then ϵ will be within 10^{-3} – 10^{-5} . We can neglect back mutation from mutant to wildtype because (before therapy) the population is dominated by wildtype virus. We assume that wildtype and mutant may differ in their rates at which they infect new cells, β and β_m , and the rates at which infected cells produce virus, k and k_m . In the absence of drug treatment the wildtype has a higher basic reproductive ratio (i.e. fitness) which implies $\beta k > \beta_m k_m$. This condition specifies that selection favours wildtype virus. The steady state of (8) is $x^* = (au)/[\beta k(1 - \epsilon)]$, $y^* = (\lambda - dx^*)/[x^*(\beta k + \beta_m k_m A)/u]$, $v^* = ky^*/u$, $y_m^* = y^* A$, $v_m^* = k_m y_m^*/u$ with $A = [\epsilon/(1 - \epsilon)]/[1 - (\beta_m k_m)/(\beta k)(1 - \epsilon)]$. For small ϵ we obtain

$$y_m^* = y^* \epsilon / \left(1 - \frac{\beta_m k_m}{\beta k}\right) \quad v_m^* = \frac{k_m}{k} v^* \epsilon / \left(1 - \frac{\beta_m k_m}{\beta k}\right) \quad (9)$$

and x^* , v^* , and y^* are very close to the corresponding values given in eqn (3).

Let us now assume that the drug completely inhibits the replication of wildtype virus ($\beta = 0$), but does not affect the mutant. (The second assumption can easily be replaced by introducing a somewhat reduced growth rate of the mutant under drug therapy; this does not change the essentials of the model.) This gives rise to the equations:

$$\begin{aligned}\dot{x} &= \lambda - dx - \beta_m xv_m \\ \dot{y} &= -ay \\ \dot{v} &= ky - uv \\ \dot{y}_m &= \beta_m xv_m - ay_m \\ \dot{v}_m &= k_m y_m - uv_m.\end{aligned}\quad (10)$$

We want to solve this system subject to the initial conditions (9), the steady state before drug treatment. Wildtype virus and infected cells decline as before; given by eqns (6) and (7). If the decay rate of free virus is much larger than the decay rates of infected and uninfected cells ($u \gg a, d$), then to a good approximation we may assume that $v_m = (k_m/u)y_m$ and the equations for the rise of resistant mutant become

$$\begin{aligned}\dot{x} &= \lambda - dx - \frac{\beta_m k_m}{u} xy_m \\ \dot{y}_m &= y_m \left(\frac{\beta_m k_m}{u} x - a \right).\end{aligned}\quad (11)$$

We rescale $\hat{x} = (d/\lambda)x$, $\hat{y}_m = y_m \beta_m / (du)$ and obtain

$$\begin{aligned}\dot{\hat{x}} &= d[1 - \hat{x}(1 + \hat{y}_m)] \\ \dot{\hat{y}}_m &= a\hat{y}_m[R_m \hat{x} - 1].\end{aligned}\quad (12)$$

Here we have defined

$$R_m = \lambda \beta_m k_m / (adu). \quad (13)$$

That is R_m is the basic reproductive ratio of the mutant resistant viral strain (we have used R_m , rather than the double subscripted R_{0m} , to avoid notational complexity in the expressions which follow). It is further useful to define

$$f = (\beta_m k_m) / (\beta k) = R_m / R_0. \quad (14)$$

The rescaled initial conditions are now—using eqns (2) and (3)—

$$\hat{x}(0) = 1/R_0 \quad \hat{y}_m(0) = \hat{\epsilon}. \quad (15)$$

Here $\hat{\epsilon}$ is defined (neglecting terms of relative order ϵ) as

$$\hat{\epsilon} = \epsilon R_m \left(1 - \frac{1}{R_0}\right) / (1 - f). \quad (16)$$

The solutions of system (12) follow along the lines of a similar mathematical system for the spread of infectious diseases in populations as analysed in Appendix C of Anderson & May (1991). There are two phases for the rise in resistant mutant. As long as \hat{y}_m is small compared to one, the system is approximately

$$\begin{aligned}\dot{\hat{x}} &= d(1 - \hat{x}) \\ \dot{\hat{y}}_m &= a\hat{y}_m(R_m\hat{x} - 1).\end{aligned}\quad (17)$$

We have

$$\hat{x}(t) = 1 - (1 - 1/R_0)e^{-dt} \quad (18)$$

$$\hat{y}_m(t) = \hat{\epsilon} \exp \left[a \left\{ (R_m - 1)t - \frac{R_m}{d} \left(1 - \frac{1}{R_0} \right) (1 - e^{-dt}) \right\} \right]. \quad (19)$$

Interestingly the resistant mutant, $\hat{y}_m(t)$, falls initially, because its abundance is at first still roughly set by the equilibrium in a mutation-selection balance. As the mutational influx from the wildtype disappears, because the drug stops wildtype replication, the mutant falls, because the uninfected cell population is at a level too low to maintain the mutant. But eventually the rise in the uninfected cell population, $\hat{x}(t)$, causes the resistant mutant to increase (once $R_m\hat{x} > 1$). Note that resistant mutant virus grows only because the uninfected cell population increases. Phase I ends when $\hat{y}_m(t)$ becomes of order unity, which for small f is (very) approximately at $t = 2/(R_md)$; for details of the analysis, see Anderson & May (1991, appendix C).

In phase II there is exponential growth of $\hat{y}_m(t)$, essentially on a $1/a$ timescale. Correspondingly $\hat{x}(t)$ will fall, and $\hat{y}_m(t)$ will peak when $\dot{\hat{y}}_m = 0$ or $\hat{x}(t) = 1/R_m$. At this point, $\hat{x}(t)$ is still decreasing, so $\hat{y}_m(t)$ will now fall (still on the time scale of $1/a$ at first), until $\hat{x}(t)$ ceases to decline when $\dot{\hat{x}} = 1/(1 + \hat{y}_m)$. At this point \hat{y}_m will be enough below unity that \hat{x} climbs again, but $R_m\hat{x} < 1$ and \hat{y}_m continues to fall. Eventually (time scale $1/d$) $\hat{x}(t)$ will climb back to $R_m\hat{x} > 1$, whereafter $\hat{y}_m(t)$ will rise and the cycle repeats. There are slowly damped oscillations eventually leading to the equilibrium $\hat{x} = 1/R_m$ and $\hat{y}_m = R_m - 1$. The damping time-scale is of the order of $\tau_d = 2/(R_md)$; in the later stages there are low amplitude oscillations of period $\tau_{osc} = 2\pi/\sqrt{ad(R_m - 1)}$.

In order to extract information about the ‘‘demographic’’ (birth and death) parameters in

eqns (8) from the available data, next we calculate the rise of resistant mutant in terms of the relative proportions of mutants among the populations of infected cells or free virus. The proportions of mutants in both these categories will rise, converging to essentially 100% during phase I of the dynamics. If R_m is significantly larger than unity, so that $dt < 1$ throughout phase I, eqn (19) can be Taylor-expanded to give

$$\hat{y}_m(t) = \hat{\epsilon} \exp[1 - (1 - f)at + \frac{1}{2}(R_m - f)adt^2 + \dots]. \quad (20)$$

Let us define $\phi(t) = y_m(t)/y(t)$, where y_m and y now refer to the absolute values, before any rescaling. We have, using eqn (16),

$$\phi(t) = \frac{y_m(0)}{y(0)} \exp[fat + \frac{1}{2}(R_m - f)adt^2 + \dots]. \quad (21)$$

Remember that $y_m(0)/y(0) = \epsilon/(1 - f)$ from eqn (19). The relative proportion of mutant virus among the infected cells is then

$$Y(t) = \frac{y_m(t)}{y_m(t) + y(t)} = \frac{\phi(t)}{\phi(t) + 1}. \quad (22)$$

Similarly, the fraction of mutant in the free virus population is

$$V(t) = \frac{v_m(t)}{v_m(t) + v(t)} = \frac{\phi(t)}{\phi(t) + (k/k_m)}. \quad (23)$$

If $k = k_m$, which means that wildtype and mutant do not differ in the rate at which infected cells produce virus, then the rise of mutant in the free virus and infected cell populations occurs simultaneously. If $k > k_m$ then the mutant rises first in the infected cell population. If $k < k_m$ (which is possible but unlikely, because the wildtype is expected to have a higher fitness) then the mutant rises first in the free virus population.

In particular, the time at which the mutant virus constitutes 50% of all infected cells, t_y , is given by the solution of

$$\phi(t_y) = 1, \quad (24)$$

with $\phi(t)$ defined by eqn (21). Under the approximation of eqn (21), t_y is given by the solution of the quadratic equation

$$\frac{1}{2}(R_m - f)adt_y^2 + fat_y - \ln[(1 - f)/\epsilon] = 0. \quad (25)$$

For specified values of the parameters R_m, f, a, d , and ϵ , the solution is routine. In the limit when R_m is significantly greater than f , a significantly larger than

d (infected cells live less long than uninfected ones), and $\epsilon \ll 1$, we have the approximate solution

$$t_y \approx (1/fa) \ln[(1-f)/\epsilon], \quad \text{if } \frac{2f^2a}{R_md} > \ln\left(\frac{1-f}{\epsilon}\right), \quad (26)$$

$$t_y \approx \sqrt{\frac{2}{R_m ad} \ln[(1-f)/\epsilon]}, \quad \text{if } \frac{2f^2a}{R_md} < \ln\left(\frac{1-f}{\epsilon}\right). \quad (27)$$

Likewise, the time at which the mutant virus represents 50% of all free virus, t_v , is given by $\phi(t_v) = k/k_m$. The approximate results of eqns (26) and (27) again pertain, except now ϵ is replaced by $\epsilon k_m/k$ in the argument of the logarithmic term.

Finally, the difference between the times when the mutant virus constitutes 50% of all infected cells, and 50% of all free virus, $\Delta = t_y - t_v$, is given under the approximation of the quadratic equation (25) for t_y , and its analogue for t_v , as:

$$\Delta = \frac{\ln(k_m/k)}{fa + \frac{1}{2}(R_m - f)ad(t_y + t_v)}. \quad (28)$$

Thus, empirical observations of t_y and t_v enable us to make inferences about the rate constants. In particular, eqn (25) or (27) may be used to obtain a rough estimate on the basic reproductive ratio, R_m , of the mutant under drug therapy. It must be kept in mind that this analysis is based on the assumption that t_y and t_v are both attained during “phase I” of the mutant virus’ dynamics (i.e., with $\hat{y}_m(t) < 1$); in any applications, either to understanding simulations or analysing real data, the validity of this approximation should be checked for consistency, once inferences have been drawn.

Figure 1 shows the dynamics of the emergence of drug-resistant virus in the basic model. In the simulation it takes about 9.7 days for the resistant virus to reach 50% prevalence in the infected cell population. This agrees well with a prediction of 10.1 days from the analytic approximation given by eqn (27).

5. Different Types of Infected Cells

In HIV infected individuals, large proportions of infected cells do not produce new virus particles. These cells can either harbour replication competent virus which is in a latent state, waiting to be reactivated, or defective virus which is unable to complete its life cycle. In addition, there are long-lived infected cells which continuously produce a small amount of new virus particles. Therefore, we now

expand the basic system (7) by including populations of long-lived infected cells that harbour latent (or chronically producing) virus and defective virus, as distinct from those with actively replicating virus. Let y_1 , y_2 , and y_3 denote infected cells that contain actively replicating virus, latent virus, and defective virus, respectively. We obtain

$$\begin{aligned} \dot{x} &= \lambda - dx - \beta xv \\ \dot{y}_i &= q_i \beta xv - a_i y_i \quad i = 1, 2, 3 \\ \dot{v} &= k y_1 + c y_2 - uv. \end{aligned} \quad (29)$$

The parameter q_i describes the probability that upon infection a cell will enter type i ; $\sum q_i = 1$. Thus q_1 is the probability that the cell will immediately enter active viral replication; y_1 cells will produce virus at rate k . The parameter q_2 is the probability that the cell will become latently infected with the virus and produce virus at a much slower rate c . In terms of this model, latent cells are in fact slow chronic producers of free virus. The parameter q_3 specifies the probability that infection of a cell produces a defective provirus that will not produce any offspring virus. The decay rates of actively producing cells, latently infected cells and defectively infected cells are a_1 , a_2 , and a_3 , respectively. From previous studies (Wei *et al.*, 1995) we know that a_1 is around 0.4 per day and a_3 around 0.01 per day. We expect a_2 to lie between these two values. The death rate of uninfected cells, d , will be similar to a_3 (probably slightly smaller).

Provided the basic reproductive ratio of the wildtype,

$$R_0 = \lambda \beta A / (du), \quad (30)$$

is larger than one, the system converges to the equilibrium

$$\begin{aligned} x^* &= u/(\beta A) \\ y_1^* &= \frac{q_1}{a_1} \left(\lambda - \frac{du}{\beta A} \right) \\ y_2^* &= \frac{a_1}{a_2} \frac{q_2}{q_1} y_1^* \\ y_3^* &= \frac{a_1}{a_3} \frac{q_3}{q_1} y_1^* \\ v^* &= \frac{\lambda}{u} A - \frac{d}{\beta} \end{aligned} \quad (31)$$

where

$$A = \frac{k q_1}{a_1} + \frac{c q_2}{a_2}. \quad (32)$$

The similarities with, and differences from, the preceding Basic Model are as we would expect.

During drug therapy ($\beta = 0$), wildtype virus will, as before, decline exponentially in the individual types of infected cells

$$y_i(t) = y_i^* e^{-a_i t} \quad i = 1, 2, 3. \quad (33)$$

Free wildtype virus particles decay according to

$$v(t) = v^* e^{-ut} + y_1^* \frac{k}{u - a_1} (e^{-a_1 t} - e^{-ut}) + y_2^* \frac{c}{u - a_2} (e^{-a_2 t} - e^{-ut}). \quad (34)$$

If u is sufficiently larger than the other decay constants, then a good approximation is

$$v(t) = y_1^* \frac{k}{u} e^{-a_1 t} + y_2^* \frac{c}{u} e^{-a_2 t}. \quad (35)$$

We know that free virus declines with a half-life of about 2 days (Wei *et al.*, 1995; Ho *et al.*, 1995; Nowak *et al.*, 1995) and hence the leading term of viral decay has to be the a_1 -exponential decline. Therefore, we conclude that most of the free plasma virus is produced by actively replicating cells. Latently

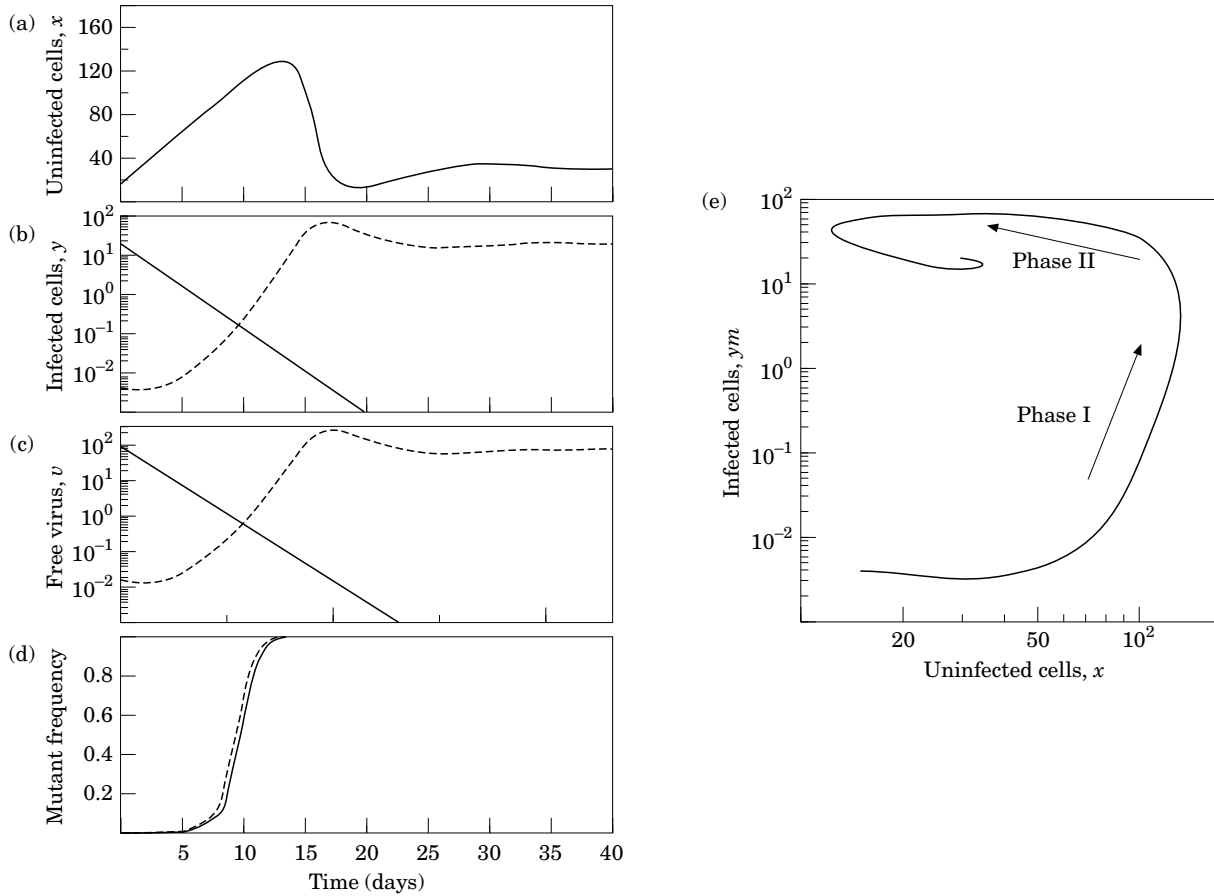


FIG. 1. A computer simulation of the basic model [eqn (8)] describing the rise of resistant mutant virus during drug therapy. Uninfected cells rise initially almost linearly with time. Wildtype virus declines exponentially with rate a both in terms of infected cells and free virus. Resistant mutant initially declines compared to its pretreatment steady state, but then rises rapidly as a consequence of an increase in uninfected cell numbers. Subsequently uninfected cells decline and the system converges to a new steady state with the virus population consisting entirely of resistant mutant. Note that new and old steady state have essentially equivalent x , y and v values, even if the replication rate of the resistant virus during drug therapy is much lower than the replication rate of wildtype virus before therapy. Parameter values are $\lambda = 10$, $d = 0.01$, $a = 0.5$, $u = 3$, $\beta = 0.01$, $\beta_m = 0.005$, $\epsilon = 0.0001$, $k = k_m = 10$ per day. This implies that the average life times of uninfected cells, infected cells and free virus are, respectively, 100, 2 and 0.333 days. The basic reproductive ratio of wildtype virus before treatment is $R_0 = 66.6$ and of resistant virus during treatment is $R_m = 33.3$. In the simulation it takes about $t_y = 9.7$ days for the resistant virus to increase to a relative frequency of 50% in the infected cell population. Using eqn (27) of our analytical approximation, we obtain $t_y = 10.1$ days; the exact solution of the quadratic eqn (25) suggests $t_y = 8.8$ days. (a) Uninfected cells, x vs. time. (b) Infected cells: wildtype virus, y continuous line; mutant virus, y_m , broken line. (c) Free virus population: wildtype virus, v , continuous line; mutant virus, v_m , broken line. (d) Relative frequency of mutant virus in free virus (continuous line) and infected cell population (broken line). (e) Phase diagram of uninfected cells, x , vs. cells infected by mutant virus, y_m . Initially the abundance of mutant virus declines, but the increase in x causes a massive proliferation of mutant virus (Phase I). The expansion of mutant virus leads after some time to a decline in uninfected cells (Phase II). Convergence to equilibrium is in damped oscillations.

infected cells can only contribute a little to the plasma virus pool; in mathematical terms we must have $ky_1^* \gg cy_2^*$.

The full dynamics, including drug-resistant strains, is described by the following system:

$$\begin{aligned}\dot{x} &= \lambda - dx - \beta xv - \beta_m xv_m \\ \dot{y}_i &= q_i \beta (1 - \epsilon) xv - a_i y_i \quad i = 1, 2, 3 \\ \dot{v} &= ky_1 + cy_2 - uv \\ \dot{y}_{im} &= q_i \beta \epsilon xv + q_i \beta_m xv_m - a_i y_{im} \quad i = 1, 2, 3 \\ \dot{v}_m &= k_m y_{1m} + c_m y_{2m} - uv_m.\end{aligned}\quad (36)$$

For a small mutation rate, ϵ (and a basic reproductive ratio larger than one), the mutant virus and its infected cells are initially present at their low, mutation-selection levels, given by putting all time derivatives equal to zero in eqn (36). Neglecting relative order ϵ , we get:

$$\begin{aligned}y_{im}^* &= \epsilon y_i^* / (1 - f) \quad i = 1, 2, 3 \\ v_m^* &= \epsilon v^* (\beta / \beta_m) f / (1 - f).\end{aligned}\quad (37)$$

Here we have, in analogy with the Basic Model, defined

$$f = R_m / R_0, \quad (38)$$

with R_0 defined by eqns (30) and (32), and R_m defined correspondingly as

$$R_m = \lambda \beta_m A_m / du. \quad (39)$$

Paralleling eqn (32), A_m is defined as

$$A_m = \frac{k_m q_1}{a_1} + \frac{c_m q_2}{a_2}. \quad (40)$$

The quantities x^* , v^* , y_i^* are defined as above, in eqns (31). These results are straightforward extensions of those for the earlier Basic Model.

We now turn to analyse the dynamics of the rise of resistant mutant virus populations, and their infected cells, following the sustained administration of drug after $t = 0$; that is, we look at eqns (36) with $\beta = 0$ for $t \geq 0$. For the following calculations we shall assume that most of the free virus is produced by the active rather than the latent cell pool. Thus, from now on, we neglect cy_2 compared with ky_1 , and similarly for the mutant. This reasonable approximation will greatly reduce the complexity of our analysis, permitting insight into the numerical simulations.

With $\beta = 0$, and $c = c_m = 0$, the dynamics of the mutant virus and the cells it infects are given, for $t > 0$, by

$$\begin{aligned}\dot{y}_{im} &= q_i (\beta_m k_m x y_{1m} / u) - a_i y_{im}, \\ \dot{x} &= \lambda - dx - (\beta_m k_m / u) y_{1m} x.\end{aligned}\quad (41)$$

As before, we assume the viral turn-over rate, u , is significantly faster than other rate constants, so that the mutant virus dynamics tracks that of y_{1m} :

$$v_m(t) \approx (k_m / u) y_{1m}(t). \quad (42)$$

It is apparent that the dynamics of $x(t)$ and $y_{1m}(t)$ are again described by the pair of equations given earlier as eqn (12):

$$\begin{aligned}\dot{\hat{x}} &= d[1 - \hat{x}(1 + \hat{y}_{1m})], \\ \dot{\hat{y}}_{1m} &= a_1 \hat{y}_{1m} [R_m \hat{x} - 1].\end{aligned}\quad (43)$$

The rescaling is exactly as in eqn (12), and R_m is defined by eqn (39) which, for $c_m = 0$, is

$$R_m = q_1 \lambda \beta_m k_m / (a_1 du). \quad (44)$$

In eqn (43), the initial conditions are again given by eqn (15). The dynamics of the population of infected cells which are actively producing virus, $y_{1m}(t)$, and consequently the dynamics of the mutant virus population itself [via eqn (42)], again follow the several phases outlined above [see paragraphs following eqn (19)]. Specifically, in phase I the population of infected cells which are actively producing viral mutants will increase as given by eqn (20):

$$\begin{aligned}\hat{y}_{1m}(t) &= \hat{\epsilon} \exp[-(1 - f)a_1 t \\ &\quad + \tfrac{1}{2}(R_m - f)a_1 dt^2 + \dots].\end{aligned}\quad (45)$$

For the pool of cells latently infected with resistant mutant virus, $y_{2m}(t)$, we have the equation

$$\dot{y}_{2m}(t) = q_2 (\beta_m k_m / u) x y_{1m} - a_2 y_{2m}. \quad (46)$$

This can be integrated to get

$$\begin{aligned}y_{2m}(t) &= y_{2m}^* e^{-a_2 t} + (q_2 \beta_m k_m / u) \\ &\quad \int_0^t x(s) y_{1m}(s) e^{-a_2(t-s)} ds.\end{aligned}\quad (47)$$

On the r.h.s., the first term is initially of order ϵ , and thereafter decreases; the second term begins of order ϵ , but increases. Henceforth we neglect this first term on the r.h.s.

Similarly, from eqn (41) we obtain for the population of defectively infected cells the approximate expression

$$y_{3m}(t) = (q_3 \beta_m k_m / u) \int_0^t x(s) y_{1m}(s) e^{-a_3(t-s)} ds. \quad (48)$$

Alternatively, expressed in terms of the rescaled \hat{x} and \hat{y}_{1m} of eqn (43), we have

$$y_{3m}(t) = q_3 \lambda \int_0^t \hat{x}(s) \hat{y}_{1m}(s) e^{-a_3(t-s)} ds. \quad (49)$$

We conclude this section with remarks on the characteristic dynamics of each of the populations of cells, y_{1m} , y_{2m} , and y_{3m} . We refer both to absolute abundance, and—in analogy to the discussion of the Basic Model—to abundance relative to (declining) populations of corresponding cells infected with the wildtype virus. The discussion is illustrated with reference to the numerical simulations of Fig. 2. Our main purpose, however, is to gain qualitative insights which may help us extract information about vital rates from empirical data on temporal abundance of uninfected and different types of infected cells.

(i) Uninfected cells, $x(t)$. With $\beta = 0$ for $t > 0$, we expect $x(t)$ to rise (at first roughly linearly, $x(t) \approx x^* + \lambda t(1 - 1/R_0) + O(t^2)$) during phase I. Eventually, $x(t)$ will damp to its asymptotic value at $x_m^* = 1/R_m$.

(ii) Infected cells, actively producing resistant mutant virus, $y_{1m}(t)$. Here we have eqn (5) as an approximate description of $y_{1m}(t)$ throughout “phase I”, where $\hat{y}_{1m} = (\beta_m k_m / du) y_{1m} < 1$. Thereafter, $y_{1m}(t)$ rises further on a fast, $1/a_1$, time-scale, and subsequently falls and further executes damped oscillations, toward an asymptotic value of $y_{1m}(\infty) = (q_1 \lambda / a_1)(1 - 1/R_m)$.

From a practical point of view, this suggests that we can estimate λ from the early (roughly linear) slope of the $x(t)$ vs t data, and thence estimate q_1/a_1 from the asymptotic value of $y_{1m}(t \rightarrow \infty)$ (assuming $1/R_m$ is smallish compared with unity).

For an estimate of $Y_1(t)$, the fraction of mutant-infected cells among the totality of actively replicating infected cells, we again have eqn (22),

$$Y_1(t) = \frac{\phi_1(t)}{\phi_1(t) + 1}. \quad (50)$$

Here $\phi_1(t) = y_{1m}(t)/y_1(t)$ is again given essentially by eqn (21), except a_1 replaces a , and R_m is given by eqn (44). The 50% point is thus again given by eqn (25):

$$\frac{1}{2}(R_m - f)a_1 dt_y^2 + fa_1 t_y - \ln[(1 - f)/\epsilon] = 0. \quad (51)$$

Thus, depending on what inferences can be drawn about parameter combinations by other means, observation of t_y from empirical data permits assessment of parameters like a_1 , f , and ϵ .

For the specific parameter values chosen in the numerical simulations of Fig. 2, we have $f = 0.5$,

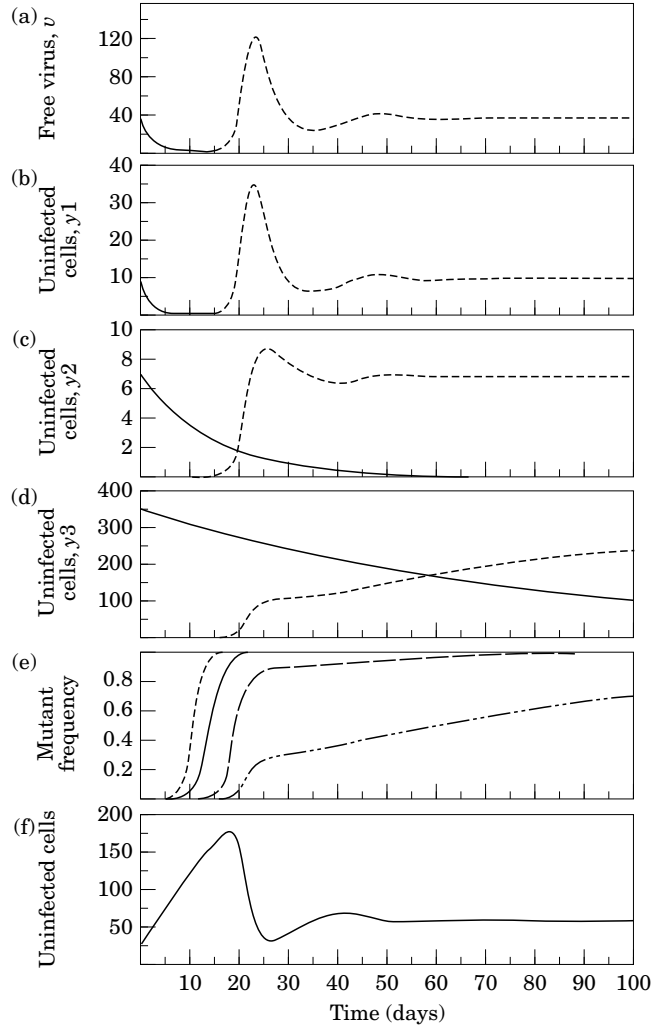


FIG. 2. Computer simulation of the extended model [eqn (36)] describing the dynamics of drug-sensitive wildtype virus and drug-resistant mutant virus in the free virus population, v , and infected cell populations harbouring replication active virus, y_1 , latent virus, y_2 , and defective virus, y_3 . The declining wildtype virus is shown by a continuous line, whereas the broken line indicates the rising mutant virus. Panel (e) shows the relative frequency of mutant virus emerging in the actively infected cell population (broken line), followed by the free virus population (continuous line), followed by the latently infected cell population (broken line long dashes) and finally followed by the defectively infected cell population (broken line with 2 short dashes 1 long dash). Panel (f) displays the dynamics of the uninfected cell population, x . Parameter values are $\lambda = 10$, $d = 0.01$, $a_1 = 0.5$, $a_2 = 0.07$, $a_3 = 0.0125$, $u = 3$, $\beta = 0.01$, $\beta_m = 0.005$, $\epsilon = 0.0001$, $k = k_m = 10$ and $c = c_m = 1$ per day. The probabilities of producing actively infected, latently infected and defectively infected cells are $q_1 = 0.5$, $q_2 = 0.05$, and $q_3 = 0.45$, respectively. Our parameter choice implies that latently infected cells have an average life-span of about 14 days, whereas defectively infected cells have an average life-span of 80 days.

$R_m = 33.3$, $a_1 = 0.5$, $d = 0.01$ and $\epsilon = 0.0001$. Here the approximate eqn (25) gives $t_y \approx 10$ days, in good agreement with the computations illustrated in Fig. 2.

Notice also in this example that $k_m = k$, whence the mutant virus—expressed as a proportion of total virus—rises almost exactly as fast as do actively-replicating infected cells. More generally, if $k_m < k$, we would see mutant virus, expressed proportionately [the V of eqn (23)], rising later than actively-replicating infected cells (the Y_1 defined above).

(iii) Defectively infected cells, $y_{3m}(t)$. Initially, the ratio $y_{3m}(0)/y_3(0)$ is $\epsilon/(1-f)$, as given by eqn (31). More generally, we can write the proportion of mutant-infected cells among all defectively-infected cells as

$$Y_3(t) = \frac{y_{3m}}{y_{3m} + y_3} = \frac{\phi_3}{\phi_3 + 1}. \quad (52)$$

Here $\phi_3(t)$ is defined, from the good approximation of eqn (49), as

$$\phi_3(t) = \frac{a_3}{(1 - 1/R_0)} \int_0^t \hat{x}(s) \hat{y}_{1m}(s) e^{a_3 s} ds. \quad (53)$$

Remember, $\hat{x}(0)\hat{y}_{1m}(0) = \epsilon f(1 - 1/R_0)/(1 - f)$.

For small t , ϕ_3 is of order ϵ . For very large t , $a_3 t \gg 1$, the non-exponential part of the integrand will asymptote to the value $\hat{x}(t)\hat{y}_{1m}(t) \rightarrow 1 - 1/R_m$; thence for $a_3 t \gg 1$ we get

$$\phi_3(t) \rightarrow \left(\frac{R_m - 1}{R_m - f} \right) e^{a_3 t}. \quad (54)$$

The passage from $\phi_3 \approx \epsilon$ to $\phi_3 \gg 1$ is, however, complex and dependent on the relative time scales involved. We have already assumed that the turn-over (death) rate of free virus is the fastest rate in the system ($u \gg a_i$ and d). We have also earlier assumed that virus-producing cells live significantly shorter than uninfected cells ($a_1 \gg d$). We now further explore the case where the death rate of defectively-infected cells, y_3 , are comparable with uninfected ones, with latent cells, y_2 , having intermediate death rates: $u \gg a_1 > a_2 \gg a_3 \approx d$.

These assumptions seem biological reasonable. They appear to accord roughly with the available data on HIV infection, and they pertain to the numerical simulations of Fig. 2. Under these assumptions, in the extreme limit where a_3 and d are so much slower than a_1 that we can regard \hat{x} and \hat{y}_{1m} as moving to their long-term equilibrium values effectively instantly (on an $1/a_3$ -time-scale), we could just write $\phi_3 \approx a_3(R_m - 1)/(R_m - f) \int_0^t e^{a_3 s} ds$. The time for 50% of all defectively-infected cells to be those infected with mutant virus, t_{y_3} , is then given via $Y_3 = 0.5$ and $\phi_3 = 1$ as

$$t_{y_3} \approx (1/a_3) \ln[1 + (R_m - f)/(R_m - 1)]. \quad (55)$$

In the usual case where R_m is significantly in excess of unity, we have the estimate

$$t_{y_3} \approx (\ln 2)/a_3. \quad (56)$$

In this event, empirical data which permit an estimate of t_{y_3} lead directly to assessment of the turnover rate for defectively-infected cells, a_3 . Notice, incidentally, that the approximate eqn (56) gives $t_{y_3} \approx 55$ days for the parameter values in Fig. 2, in excellent agreement with the numerical computations.

More generally, we will often have cases where, although a_3 is significantly larger than a_1 , we cannot accurately regard $\hat{x}\hat{y}_{1m}$ to attain their asymptotic values effectively instantaneously in eqn (53). Turning back to the discussion following eqns (18, 19), we can offer some rough insights. Phase I of the $\hat{x} - \hat{y}_{1m}$ dynamics lasts for a time roughly of order $1/R_m d$, and at the end of this phase \hat{x} is of order $1/R_m$ and \hat{y}_{1m} is of order 1. So we could say that after $t \approx 1/R_m d$, ϕ_3 is roughly of order (a_3/dR_m^2) , or $1/R_m^2$ if a_3 and d are comparable. In phase II, \hat{x} remains very roughly of order $1/R_m$, while \hat{y}_{1m} gets significantly larger than unity; all this is on a timescale of order $1/a_1$. So the contribution to ϕ_3 from phase II is of general order of a_3/a_1 , which is small. Overall, this points to the approximation of eqns (55) or (56) being reasonably accurate, so long as $a_3 \gg a_1$ and $R_m d$ (which implies the requirement that R_m be significantly larger than unity). Figure 2 bears this out: the early stages of y_3 do show some of the features of y_1 , but they settle relatively quickly on the time-scale of the y_3 dynamics.

(iv) Latently infected cells, y_{2m} . Here we have expressions for the absolute number of such cells infected with mutant virus, $y_{2m}(t)$, and for the proportion of these mutant virus infected cells among all such latent cells, $y_2(t) = y_{2m}/(y_2 + y_{2m})$. These expressions are exactly as in eqns (52–56) above, with all subscripts “3” replaced by “2”.

The analysis is, however, not usually as transparent as it can be for y_{1m} and y_{3m} . If a_2 is of the order of a_1 , so that latent cells infected with mutant virus come to preponderate within the “phase I” stage of the growth of y_{1m} , then analytic approximations to eqn (53) can be constructed; in essentials, the curve for $Y_2(t)$ behave similarly to that for $Y_1(t)$. At the opposite extreme, if a_2 is of the order of a_3 , then all the remarks just made about y_3 and y_{3m} pertain equally to y_2 and y_{2m} .

Most likely, however, a_2 will lie at values intermediate between a_1 and a_3 , such that nothing simple can be said about the dynamics of $Y_2(t)$. This

is the case for the parameter values illustrated in Fig. 2.

(v) Total abundance of infected cells. Any interpretation of the dynamics of the total population of cells infected with mutant virus, $y_m(t) = y_{1m}(t) + y_{2m}(t) + y_{3m}(t)$, will depend significantly upon the factors which affect their initial relative abundances, and their asymptomatic relative abundances. For the total proportion of mutant-infected cells among all infected cells, $Y(t) = y_m(t)/[y(t) + y_m(t)]$, patterns will further depend on the initial relative abundances of the wildtype-infected cells. Insofar as a_3 is typically much smaller than a_1 and a_2 , defective cells are likely to be the most abundant of wild-type infected cells at $t = 0$. These cells, moreover, decay slowly (as $e^{-a_3 t}$), and so the rise in $Y(t)$ is likely to be dominated by the asymptotic phase of $y_m(t)$; although $Y_1(t)$ saturates to unity relatively fast, by virtue of the fast decay in $y_1(t)$ (scaling as $e^{-a_1 t}$), this does not contribute much to the larger picture of all cells, dominated by the relatively large initial number and slow decay of y_3 -cells. Such general observations again help us to interpret the trends shown in the numerical simulations.

6. Experimental Results

Three patients were treated with the reverse transcriptase inhibitor Nevirapine (NVP) (Shaw *et al.*, in preparation). Plasma virus load, CD4 cell counts and infected PBMC were measured sequentially after the start of therapy. We determined the amount of proviral DNA in peripheral blood mononuclear cells (PBMC), which gives the total proportion of HIV-infected PBMC. Using a limiting dilution assay for quantifying infectious units per 10^6 PBMC we determined the frequency of cells that harbour replication competent virus (either latently or actively replicating). In all three compartments (plasma virus, infectious PBMC and total infected PBMC) we quantify the proportions of NVP-sensitive wildtype virus and NVP-resistant mutant virus at day 0, 14, 28, 42 and 140 after initiating therapy (Fig. 3).

Table 1 gives information on viral load in terms of free virus and infected cells in 1 ml of blood in all three patients before start of therapy. Note that most HIV-infected PBMC appear to harbour replication defective virus; there are only between 15 and 30 infectious units within PBMC in 1 ml blood, but between 420 and 550 PBMC carrying HIV provirus.

In terms of our expanded model the data on proviral DNA provide information on the sum $y_1 + y_2 + y_3$, whereas the cells harbouring replication competent virus describe $y_1 + y_2$. Unfortunately, we

do not have direct experimental data on y_1 or y_2 alone. In addition, we have to bear in mind that most HIV-infected cells and perhaps also most cells that produce plasma virus are in the lymph system and not in the peripheral blood.

After start of therapy, plasma virus load declines rapidly within the first 2 weeks and subsequently increased with the emergence of resistant virus. In patients 1625 and 1605 the initial decay of wildtype plasma virus between day 0 and 14 occurs with a half-life of 2.6 and 2.1 days respectively. Over the same time infected PBMC that harbour replication

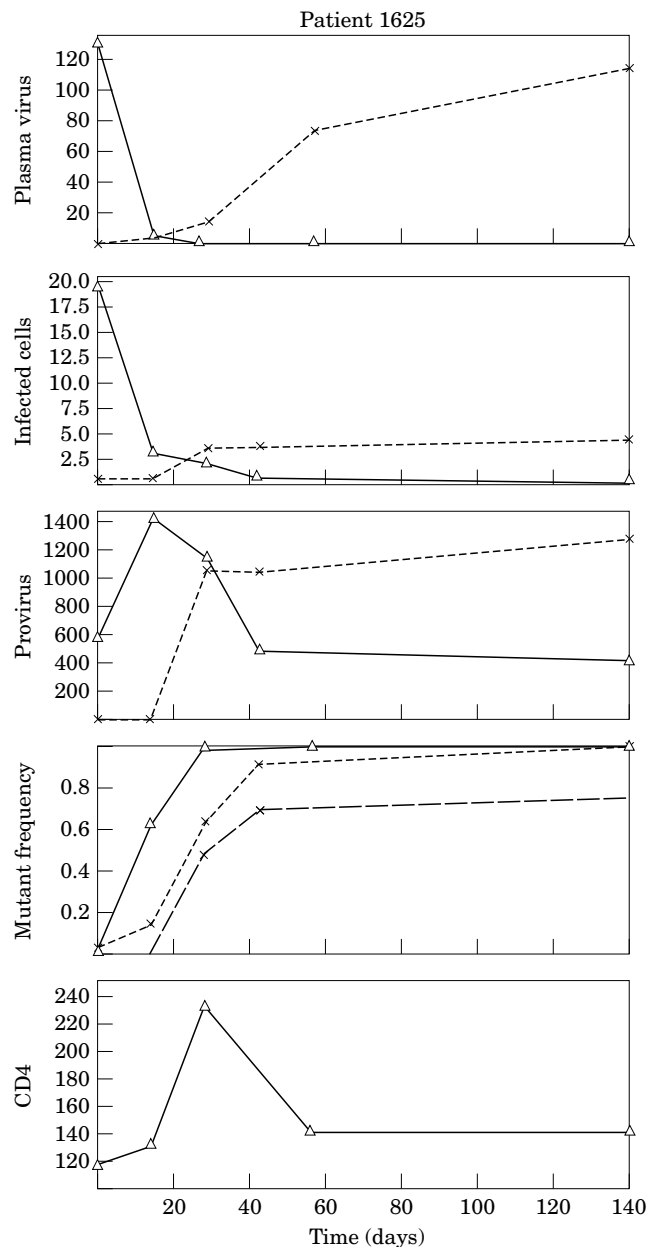


FIG. 3.(a)

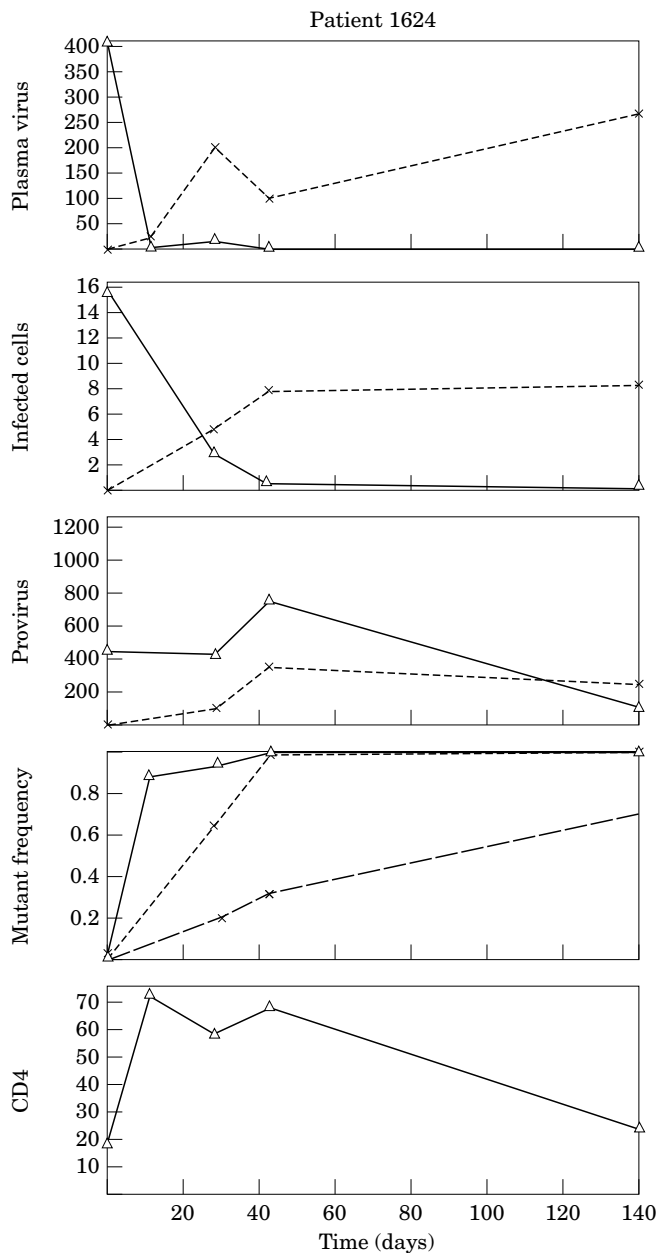


FIG. 3(b).

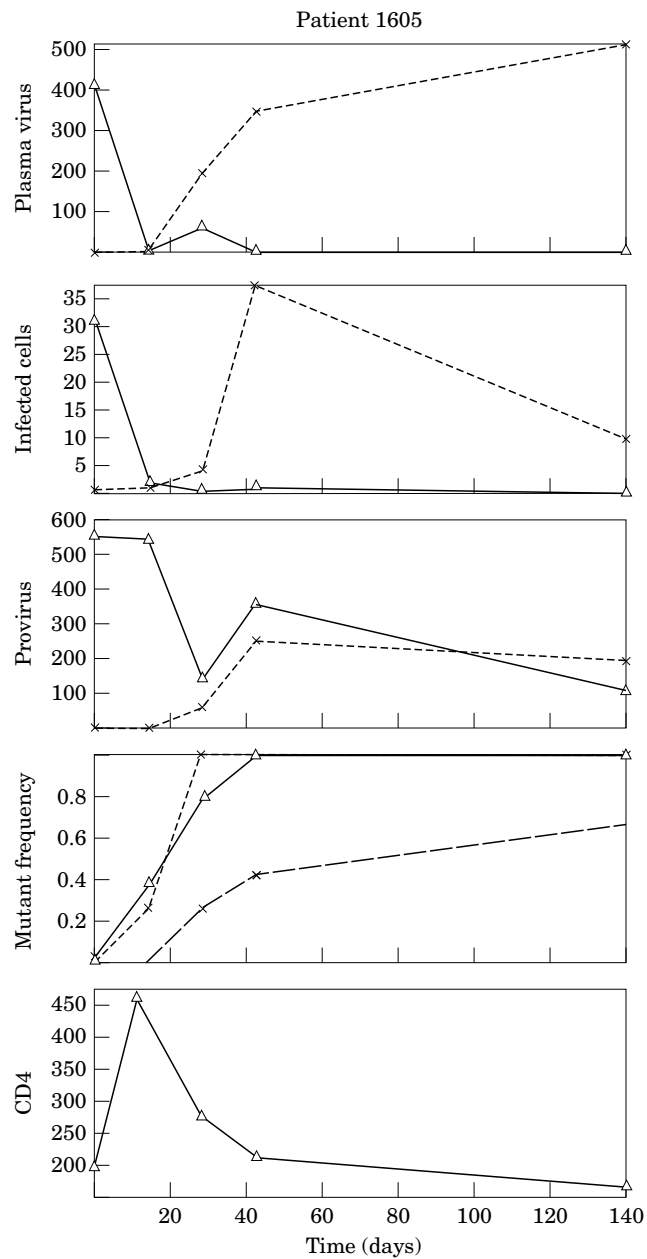


FIG. 3(c)

FIG. 3. Experimental data from three patients treated with the anti-HIV drug nevirapine. "Plasma virus" denotes free virus particles in 1 μ l plasma. "Infectious cells" denotes PBMC harbouring replication competent HIV (per 1 ml blood). "Provirus" denotes number of PBMC with HIV proviral DNA (per 1 ml blood). The continuous line is drug-sensitive wildtype virus, whereas the broken line denotes drug-resistant mutant virus. "Mutant frequency" shows the rise of NVP-resistant mutant in the free virus population (continuous line), in the infectious PBMC population (broken line short dashes) and in the total infected PBMC population (broken line long dashes). In patients 1625 and 1624 resistant mutant rises first in the plasma population and then in the infected cell population (that has infectious virus). In patient 1605 the rise appears to be more or less simultaneous. In all three patients it takes much longer for the resistant mutant to establish itself in the provirus population. CD4 cell counts are shown per 1 μ l blood.

competent wildtype virus decay only with half-lives of, respectively, 4.8 and 3.0 days. This suggests that infected PBMC contain a subset of cells with a longer half-life than those cells which produce the majority

of plasma virus. Between days 14 and 42, infected PBMC with replication competent wildtype virus decline with half-lives of 9.7 days in patient 1625 and 21 days in patient 1605. If we assume that by day 14

TABLE 1
Pretreatment data from three patients

Patient	1 ml blood contains:				
	CD4 cells	Total PBMC	Infected PBMC (provirus)	Infected PBMC (infectious virus)	Plasma virus
1625	116000	1150000	550	20	131000
1605	205000	1750000	540	31	407000
1624	19000	526000	420	16	402000

Three patients, pretreatment data.

The table shows CD4 cells peripheral blood mononuclear cells (PBMC) and virus population size in terms of infected cells and free virus. "Infected PBMC (provirus)" denotes cells that harbour HIV DNA in their genome. "Infected PBMC (infectious virus)" denotes cells that contain replication competent HIV. Note that the large majority of infected cells (more than 90%) appears to be unable to produce infectious virus upon stimulation in vitro. "Plasma virus" denotes free virus particles.

actively infected cells with wild-type virus (half-life of about 2 days) have essentially disappeared, we can use these estimates to extrapolate backwards in time and estimate what fraction of cells were latently infected at day 0. For patient 1625 we obtain that about 40% of PBMC with replication competent virus were latently infected, which is about 7 in 10^6 PBMC. For patient 1605 we obtain 7% which comes to about 1 in 10^6 PBMC. For patient 1624 these calculations are not possible because we lack measurements for day 14. Table 2 shows the relative abundance of total infected cells, actively infected cells and latently infected cells in the PBMC population.

NVP-resistant virus rises rapidly in all three patients in the free plasma virus population followed with a small delay in infected cells harbouring replication competent virus and with considerable

delay in infected cells harbouring HIV provirus (Fig. 3). At day 28 plasma virus contains 100% resistant virus in patients 1625, 76% in patient 1605 and 92% in patient 1624. It takes between 10 and 20 days for the resistant virus to reach 50% prevalence in the free virus population.

Using eqn (27) we can get a very crude estimate for the basic reproductive ratio of the resistant mutant under drug therapy. From eqn (27) we obtain $R_m = \alpha/t_y^2$ with $\alpha = (2/ad)\ln[(1-f)/\epsilon]$. Assuming $a = 0.5$, $d = 0.01$, $\epsilon = 0.0001$ and f somewhere between 0 and 0.99 we get $\alpha \approx 2000-4000$. If we take the rise of resistant mutant in the free virus population as indicative of the rise in the actively virus producing infected cell population, i.e. $t_y \approx t_v$ (which holds if $k \approx k_m$), then an experimental observation of $t_v \approx 10$ days suggests a basic reproductive ratio of $R_m \approx 20-40$. Thus the intrinsic growth rate of the NVP-resistant mutant virus if target cell availability was not limiting may be between 20 and 40 infected cells arising from any one infected cell. This estimate is of course only very crude.

NVP-resistant mutant rises only slowly in the DNA provirus population. After 140 days between 65% and 75% of infected PBMC harbour mutant provirus, which suggests that the turnover rate of infected PBMC at large is slow (see also Wei *et al.*, 1995). Using eqn (56) we obtain an average half-life of about 80 days for infected PBMC. The time lag between viral variants that emerge in the plasma RNA population and the proviral DNA population has also previously been noted by studies of HIV evolution in single patients (Simmonds *et al.*, 1991).

We can also obtain a very crude estimate of the probability that infection of a cell will result in

TABLE 2
Relative amounts of HIV-infected PBMC in three patients before drug treatment

Patient	1 million PBMC contain:		
	Infected PBMC (provirus)	Infected PBMC (infectious virus)	Infected PBMC (latent virus)
1625	480	17	7
1605	310	18	1
1624	800	29	N/A

Three patients, pretreatment data.

"Infected PBMC (provirus)" denotes cells that harbour HIV DNA in their genome. "Infected PBMC (infectious virus)" denotes cells that contain replication competent HIV, which can either be active or latent. "Infected PBMC (latent virus)" denote cells that harbour replication competent, but latent virus. This number is estimated and can only be seen as a very rough guide (see main text). The estimate of latently infected cells is not possible for patient 1624.

defective or replication competent provirus. In analogy to eqn (31) we obtain

$$\frac{A_1 Y_1}{Q_1} = \frac{A_2 Y_2}{Q_2}, \quad (57)$$

where A_1 denotes the average death rate of a cell harbouring replication competent virus and A_2 is the death rate of defectively infected cells. Q_1 and Q_2 are the probabilities that infection of a cell (defined as establishment of a provirus) has lead to a replication competent or defective provirus, respectively. Clearly, $Q_1 + Q_2 = 1$. Y_1 and Y_2 are number of cells harbouring replication competent and defective provirus, respectively. We have direct information on Y_1 and Y_2 before start of therapy. We estimate A_1 from the decline of infected PBMC harbouring replication competent wildtype virus and A_2 from the decline of defectively infected PBMC. Thus we obtain Q_1 and Q_2 . In all patients A_2 is approximately 0.0086 per day which is equivalent to a half-life of 80 days. For patient 1625 we have $Y_1 = 17$, $Y_2 = 463$ and calculate $A_1 = 0.15$ per day. This leads to $Q_1 = 0.2$ and $Q_2 = 0.8$. For patient 1605 we have $Y_1 = 18$, $Y_2 = 292$ and calculate $A_1 = 0.23$, leading to $Q_1 = 0.22$ and $Q_2 = 0.78$. For patient 1624 this analysis gives $Q_1 = 0.37$. Therefore, it seems that if infection of a cell leads to a provirus the chance is between 0.2 and 0.4 that this provirus is replication competent. The fact that the large majority of infected PBMC harbour defective provirus is mostly a consequence of their slow turnover rate.

7. Conclusions

We have developed a mathematical framework for studying the emergence of resistant mutant virus during drug treatment. We assume that mutant virus exists already before start of therapy and is held in a mutation-selection equilibrium. Without drug the fitness of wildtype is higher than the fitness of mutant, but continuous mutation of wildtype virus (together with replication of mutant virus) produces a small amount of mutant virus. The frequency of resistant mutant virus before therapy is given by

$$v_m/v = \epsilon/(1 - R_m/R_0). \quad (58)$$

Here ϵ is the mutation probability from wildtype to mutant, R_0 is the basic reproductive ratio (i.e. fitness) of wildtype virus and R_m is the basic reproductive ratio of mutant virus—both before therapy. [We have also assumed that both wildtype and mutant have the same rate of virus production from infected cells, i.e. $k = k_m$. Otherwise see eqn (9).] If the fitness of the mutant is much smaller than that of the wildtype

($R_m \ll R_0$), then the frequency of the mutant virus is given by the mutation rate, ϵ . If on the other hand, the fitnesses of wildtype and mutant are quite similar, then also the denominator in eqn (58) plays an important role. For example, if mutant and wildtype differ in a single point mutation, if the point mutation rate is 10^{-4} , and if $R_m = 0.9R_0$, the pre-treatment frequency of resistant mutant is 10^{-3} .

Our analytic approximation for the emergence of resistance rests on the assumption that resistant virus rises as a consequence of increased abundance of target cells (McLean & Nowak, 1992). From eqn (20) we have

$$v_m(t) \approx v_m(0)\exp[-(1 - R_m/R_0)at + \frac{1}{2}R_m(1 - 1/R_0)adt^2 + \dots]. \quad (58)$$

Here $v_m(t)$ is the abundance of mutant virus at time t after start of therapy, while a and d denote death rates of infected and uninfected cells. Thus monitoring the rise of resistant mutant during drug therapy provides information on the basic reproductive ratio of HIV during infection. Note that this equation simply describes the rise of an already pre-existing mutant virus. If several mutations are necessary to confer resistance and if this involves complex evolutionary changes in the virus genome, then eqn (58) is not valid.

Our mathematical model in conjunction with data from three patient treated with the anti-HIV drug nevirapine also provides new insights into the in vivo kinetics of HIV turnover. Together with previous work (Ho *et al.*, 1995; Wei *et al.*, 1995; Coffin, 1995; Nowak *et al.*, 1995; Perelson *et al.*, 1996), the following picture has emerged: most of plasma virus is produced by cells with a half-life of about 1.5 to 2 days; latently infected cells have a half-life of about 10 to 20 days (but much more information is needed here to derive more accurate figures); most infected peripheral blood mononuclear cells (PBMC) harbour replication defective provirus and have a half-life of about 80 days; free plasma virus has a half-life of less than 6 hr.

It is still an open question how this kinetic picture of HIV infection ties in with the dynamics of disease progression. Virus load (i.e. the abundance of free virus in plasma) has been shown to be an important determinant of disease progression; patients with a high virus load soon after primary infection progress faster to AIDS than patients with a low virus load (Mellors *et al.*, 1996; Ho, 1996). Several factors, which can be host and virus specific, determine virus load, among these are the replication ability of the virus (Deacon *et al.*, 1995), the activation state of the

CD4 cell population (note that HIV replicates predominantly in activated CD4 cells), and immune responsiveness, defined as the patients ability to mount an immune response to the virus (Nowak & Bangham, 1996). Mathematical models of disease progression have to deal with the problem how the steady state of HIV-1 short-term kinetics is shifted toward higher virus load and lower CD4 cell abundance. Possible explanations include virus evolution (Nowak *et al.*, 1990, 1991, 1995; deBoer & Boerlijst, 1994; Nowak & McMichael, 1995), a slow destruction of the immune response against HIV, or increased levels of target cell activation (McLean & Nowak, 1992).

Support from the Wellcome Trust (MAN, SB) and the Royal Society (SB, RMM) is gratefully acknowledged.

REFERENCES

- ANDERSON, R. M. & MAY, R. M. (1991). *Infectious Diseases of Humans*. Oxford: Oxford University Press.
- BOUCHER, C. A., TERSMETTE, M., LANGE, J. M., KELLAM, P., DE GOEDE, R. E., MULDER, J. W., *et al.* (1990) Zidovudine sensitivity of human immunodeficiency viruses from high-risk, symptom-free individuals during therapy. *Lancet* **336**(8715), 585–90.
- BOUCHER, C. A., LANGE, J. M., MIEDEMA, F. F., WEVERLING, G. J., KOOT, M., MULDER, J. W., *et al.* (1992) HIV-1 biological phenotype and the development of zidovudine resistance in relation to disease progression in asymptomatic individuals during treatment. *AIDS* **6**, 1259–1264.
- BOUCHER, C. A., O'SULLIVAN, E., MULDER, J. W., RAMAUTARSING, C., KELLAM, P., DARBY, *et al.* (1992). Ordered appearance of zidovudine resistance mutations during treatment of 18 human immunodeficiency virus-positive subjects. *J. Infect. Dis.* **165**(1), 105–110.
- COFFIN, J. M. (1995). HIV population dynamics in vivo: implications for genetic variation, pathogenesis, and therapy. *Science* **267**, 483–489.
- DEACON, N. J., TSYKIN, A., SOLOMON, A., SMITH, K., LUDFORD-MENTING, M., HOOKER, D. J., *et al.* (1995). Genomic structure of an attenuated quasi species of HIV-1 from a blood transfusion donor and recipients. *Science* **270**, 988–991.
- DE BOER, R. J. & BOERLIJST, M. C. (1994). Diversity and virulence thresholds in AIDS. *Proc. Natl. Acad. Sci. USA* **94**, 544–548.
- DE BOER, R. J. & BOUCHER, C. A. B. (1996) Anti-CD4 therapy for AIDs suggested by mathematical models. *Proc. R. Soc. Lond. B*, **263**, 899–905.
- DE JONG, M. D., VEENSTRA, J., STILIANAKIS, N. I., SCHURMAN, R., LANGE, J. M. A., DE BOER, R. J. & BOUCHER, C. A. B. (1996). Host-parasite dynamics and outgrowth of virus containing a single K70R amino acid change in reverse transcriptase are responsible for the loss of HIV-1 RNA load suppression by zidovudine. *Proc. Natl. Acad. Sci. USA*, in press.
- ERON, J. J., BENOIT, S. L., JEMSEK, J., MACARTHUR, R. D., SANTANA, J., QUINN, J. B. *et al.* (1995) Treatment with lamivudine, zidovudine or both in HIV-positive patients with 200 to 500 CD4 cells per cubic millimeter. *New Eng. J. Med.* **333**, 1662–1669.
- FROST, S. D. W. & MCLEAN, A. R. (1994) Quasispecies dynamics and the emergence of drug resistance during zidovudine therapy of HIV infection. *AIDS* **8**, 323–332.
- HERZ, A. V. M., BONHOEFFER, S., ANDERSON, R. M., MAY, R. M. & NOWAK, M. A. (1996). Viral dynamics in vivo: limitations on estimates of intracellular delay and virus decay. *Proc. Natl. Acad. Sci. USA* **93**, 7247–7251.
- HO, D. D., TOYOSHIMA, T., MO, H., KEMPF, D. J., NORBECK, D., CHEN, C. M., *et al.* (1994). Characterization of human immunodeficiency virus type 1 variants with increased resistance to a C2-symmetric protease inhibitor. *J. Virol.* **68**, 2016–2020.
- HO, D. D., NEUMANN, A. U., PERELSON, A. S., CHEN, W., LEONARD, J. M. & MARKOWITZ, M. (1995). Rapid turnover of plasma virions and CD4 lymphocytes in HIV-1 infection. *Nature*. 1995 Jan 12; **373**(6510): 123–126.
- HO, D. D. (1996). Viral counts count in HIV infection. *Science* **272**, 1124–1125.
- KLEINERMAN, P., PHILLIPS, R. E., RINALDO, C. R., MCMICHAEL, A. J. & NOWAK, M. A. (1996). CTL-mediated lysis and viral turnover in HIV-1 infection, submitted.
- KIRSCHNER, D. E. & WEBB, G. F. (1996). Effects of drug resistance on monotherapy treatment of HIV infection. *J. theor. Biol.*, in press.
- LARDER, B. A., DARBY, G. & RICHMAN, D. D. (1989). HIV with reduced sensitivity to zidovudine (AZT) isolated during prolonged therapy. *Science* **243**, 1731–1734.
- LARDER, B. A. & KEMP, S. D. (1989). Multiple mutations in HIV-1 reverse transcriptase confer high-level resistance to zidovudine (AZT). *Science* **246**, 1155–1158.
- LARDER, B. A., KELLAM, P. & KEMP, S. D. (1993). Convergent combination therapy can select viable multidrug-resistant HIV-1 in vitro. *Nature* **365**, 451–453.
- LARDER, B. A., KEMP, S. D. & HARRIGAN, P. R. (1995). Potential mechanism for sustained antiretroviral efficacy of AZT-3TC combination therapy. *Science* **269**, 696–699.
- LOVEDAY, C., KAYE, S., TENANT-FLOWERS, M., SEMPLE, M., AYLIFFE, U., WELLER, I. V. & TEDDER, R. S. (1995). HIV-1 RNA serum-load and resistant viral genotypes during early zidovudine therapy. *Lancet* **345**, 820–824.
- MARKOWITZ, M., MO, H., KEMPF, D. J., NORBECK, D. W., BHAT, T. N., ERICKSON, J. W. & HO, D. D. (1995). Selection and analysis of human immunodeficiency virus type 1 variants with increased resistance to ABT-538, a novel protease inhibitor. *J. Virol.* **69**, 701–706.
- MCLEAN, A. R., EMERY, V. C., WEBSTER, A. & GRIFFITHS, P. D. (1991). Population dynamics of HIV within an individual after treatment with zidovudine. *AIDS* **5**, 485–489.
- MCLEAN, A. R. & NOWAK, M. A. (1992). Interactions between HIV and other pathogens. *J. theor. Biol.* **155**, 69–86.
- MCLEAN, A. R. & NOWAK, M. A. (1992). Competition between zidovudine sensitive and resistant strains of HIV. *AIDS* **6**, 71–79.
- MCLEAN, A. R. & FROST, S. D. W. (1995). Zidovudine and HIV: mathematical models of within-host population dynamics. *Reviews in Medical Virology* **5**, 141–147.
- MELLORS, J. W., RINALDO, C. R., GUPTA, P., WHITE, R. M., TODD, J. A. & KINGSLEY, L. A. (1996). Prognosis in HIV-1 infection predicted by the quantity of virus in plasma. *Science* **272**, 1167–1170.
- MOHRI, H., SINGH, M. K., CHING, W. T. & HO, D. D. (1993). Quantitation of zidovudine-resistant human immunodeficiency virus type 1 in the blood of treated and untreated patients. *Proc. Natl. Acad. Sci. USA* **90**, 25–29.
- NOWAK, M. A., MAY, R. M. & ANDERSON, R. M. (1990). The evolutionary dynamics of HIV quasispecies and the development of immunodeficiency disease. *AIDS* **4**, 1095–1103.
- NOWAK, M. A., ANDERSON, R. M., MCLEAN, A. R., WOLFS, T., GOUDSMIT, J. & MAY, R. M. (1991). Antigenic diversity thresholds and the development of AIDS. *Science* **254**, 963–969.
- NOWAK, M. A., MAY, R. M., PHILLIPS, R. E., ROWLAND-JONES, S., LALLOO, D. G., MCADAM, S., *et al.* (1995). Antigenic oscillations and shifting immunodominance in HIV-1 infections. *Nature* **375**, 606–611.
- NOWAK, M. A. & MCMICHAEL, A. J. (1995). How HIV defeats the immune system. *Scientific American* **273**, 58–65. August 1995.
- NOWAK, M. A., BONHOEFFER, S., LOVEDAY, C., BALFE, P., SEMPLE, M., KAYE, S., *et al.* (1995). HIV-1 dynamics: Results confirmed. *Nature* **375**, 193.
- NOWAK, M. A. & BANGHAM, C. R. M. (1996). Population

- dynamics of immune responses to persistent viruses. *Science* **272**, 74–79.
- PERELSON, A. S., NEUMANN, A. U., MARKOWITZ, M., LEONARD, J. M. & HO, D. D. (1996). HIV-1 dynamics *in vivo*: virion clearance rate, infected cell lifespan, and viral generation time. *Science* **271**, 1582–1585.
- RICHMAN, D. D. (1990). Zidovudine resistance of human immunodeficiency virus. *Rev. Infect. Dis.* **12** Suppl. 5, S507–510.
- RICHMAN, D. D., HAVLIR, D., CORBEIL, J., LOONEY, D., IGNACIO, C., SPECTOR, S. A., *et al.* (1994). Nevirapine resistance mutations of human immunodeficiency virus type 1 selected during therapy. *J. Virol.* **68**, 1660–1666.
- RICHMAN, D. D. (1994). Drug resistance in viruses. *Trends Microbiol.* **2**, 401–407.
- SCHUURMAN, R., NIJHUIS, M., VAN LEEUWEN, R., SCHIPPER, P., DE JONG, D., COLLIS, P., *et al.* (1995). Rapid changes in human immunodeficiency virus type 1 RNA load and appearance of drug-resistant virus populations in persons treated with lamivudine (3TC). *J. Infect. Dis.* **171**, 1411–1419.
- SIMMONDS, P., ZHANG, L. Q., MCOMISH, F., BALFE, P., LUDLAM, C. A. & BROWN, A. J. (1991). Discontinuous sequence change of human immunodeficiency virus (HIV) type 1 env sequences in plasma viral and lymphocyte-associated proviral populations *in vivo*: implications for models of HIV pathogenesis. *J. Virol.* **65**(11), 6266–6276.
- STASZEWSKI, S. (1995). Zidovudine and lamivudine: results of phase III studies. *J. Acquir. Immune Defic. Syndr. Hum. Retrovirol.* **10** Suppl. 1, S57.
- ST. CLAIR, M. H., MARTIN, J. L., TUDOR-WILLIAMS, G., BACH, M. C., VAVRO, C. L., KING, D. M., *et al.* (1991). Resistance to ddI and sensitivity to AZT induced by a mutation in HIV-1 reverse transcriptase. *Science* **253**, 1557–1559.
- WEI, X., GHOSH, S. K., TAYLOR, M. E., JOHNSON, V. A., EMINI, E. A., DEUTSCH, P., *et al.* (1995). Viral dynamics in HIV-1 infection. *Nature* **373**, 117–122.
- WEIN, L. M., ZENIOS, S. & NOWAK, M. A. (1997). Dynamic multidrug therapies for HIV: a control theoretic approach. *J. theor. Biol.*, in press.